SHORT COMMUNICATION

Modelling of an HTGR steam power plant

Asok Ray
Department of Mechanical Engineering, Carnegie-Mellon University, Pittsburgh, Pennsylvania 15213, USA
(Received 2 November 1978; revised 12 January 1979)

Introduction

Nuclear power plants for large-scale electric power generation are of the pressurized water reactor (PWR) and boiling water reactor (BWR) types. They have low thermal efficiencies (≅30%) in comparison to fossil-fuelled plants. This deficiency is a motivation for high temperature gas-cooled reactor (HTGR) plants, in which steam conditions and thermal efficiency (≅40%) are comparable to those in fossil-fuelled plants.

HTGR systems have been under development in Europe and the USA for more than 20 years. The first HTGR steam power plant – the 40 MW(e) pilot plant at Peach Bottom, PA., USA – was put into operation in 1967. Although cost escalation and other difficulties have resulted in indefinite deferral of 1160 MW(e) HTGR projects,[1] a 330 MW(e) HTGR demonstration plant is now in the power escalation stage at Fort St Vrain, near Denver, Colorado, USA.

HTGR plants are expected to meet the energy needs in the not too far future. However, the control problems associated with HTGR systems are complex. *A priori* analytical studies are essential for design and development of full-scale HTGR plants. Advanced analytical techniques, such as mathematical modelling and simulation are required.[2]

A nonlinear dynamic model was formulated for an 1160 MW(e) HTGR steam power plant, formerly scheduled to be built at the Fulton Station of the Philadelphia Electric Company.[3,4] The model provides the basis for (a), understanding the complex process dynamics; (b), control system design, and (c), system dynamic performance evaluation. The modelling methodology described here has general applicability, and can be readily adapted to the study of other gas-cooled steam power plants.

Modelling approach

The physical process consists of distributed parameter dynamic elements, represented by a set of nonlinear partial differential equations with space and time as independent variables. To obtain a numerical solution, these partial differential equations were approximated via spatial discretization by a finite number of ordinary differential equations with time as the independent variable. This approach has been shown to be adequate for other power generation systems by experimental verification.[5–7]

For the purpose of model development the complete plant was partitioned into several blocks as shown in *Figure 1* (see nomenclature for symbol description). Each block represented a physical component or a group of components. The lines interconnecting the blocks indicate the direction of information flow or 'model causality'. The task of modelling was then accomplished in two steps: first, modelling of each block; and second, interconnection of component models (of each block) with consistent causality.

Step 1 included determination of steady-state solutions and system eigenvalues of individual components linearized at a number of operating levels. The steady-state model results were verified with design data, and the eigenvalues were examined for frequency range. Step 2 incorporated sequential interconnection of component models. Steady-state solutions and eigenvalue sets of the augmented were examined at each phase of interconnection.

In addition to steady-state evaluation and eigenvalue determination, the family of linearized models were tested for controllability and observability with respect to a given set of control and output variables, respectively. This set of controllable and observable state variable structure allows design of a multivariable controller in the time- or frequency-domain.

The following equations were used to formulate the dynamic model: fundamental equations of mass, momentum and energy conservation; semi-empirical relationships for fluid flow and heat transfer; neutron kinetic equations; and state relations for thermodynamic properties of the working fluids. Major assumptions in addition to lumped parameter approximation were: uniform fluid flow across any cross-section; negligible axial heat transfer in working fluids, tube wall and reactor core; negligible flow inertia of helium (primary coolant) and steam; and negligible pressure drop due to velocity and gravitational heads in helium and steam paths.

The model was developed for normal operation of the HTGR power plant. Derivation of model equations and the basis for state variable selection are available elsewhere[4]; they could not be presented in this paper due to sheer bulk.

Results

The model consists of 40 first-order nonlinear ordinary time-invariant differential equations. They are arranged in state-space form to facilitate simulation and control system design. A list of state, output and input (control) variables is given in Appendix. In addition to transient response simulation, the nonlinear model was linearized at several steady-state operating conditions to examine local stability,

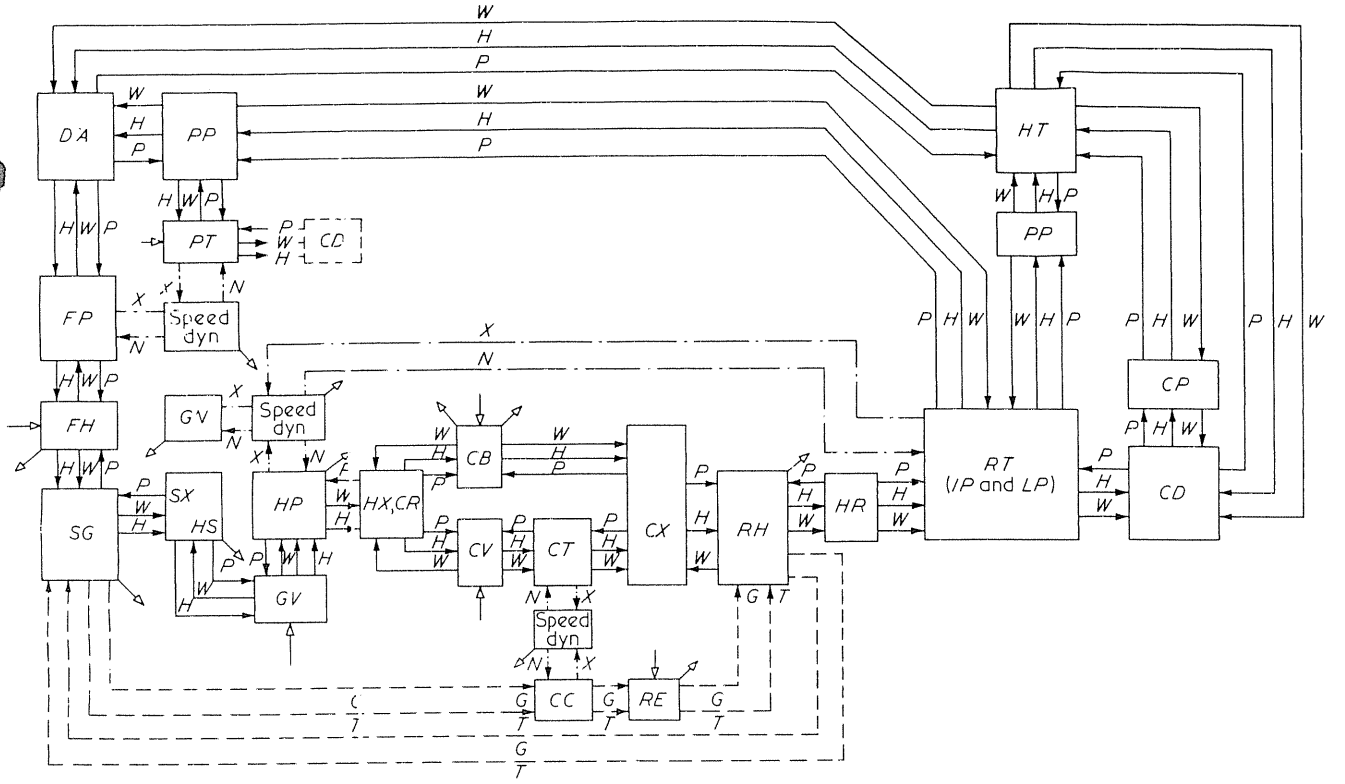

Figure 1 Model solution diagram. (→), model input; (←), model output; (—▷), controlled variable; (◁—), measured variable; (——), H_2O path; (– – –), gas path; (— · —), mechanical coupling; G, mass flow rate of gas; H, specific enthalpy; N, angular speed; P, pressure; T, temperature; W, mass flow rate of H_2O; X, torque; CB, Helium circulator turbine bypass valve; CC, Helium circulator compressor; CD, Condenser; CP, Condensate pump; CR, Cold reheat header; CT, Helium circulator turbine; CV, Helium circulator turbine steam admission valve; CX, Helium circulator turbine exhaust; DA, Deaerator; FH, Feedwater header including trim valve; FP, Feedwater pump; GN, Electrical generator; GV, High-pressure turbine governor valves; HP, High-pressure turbine; HR, Hot reheat header; HS, Main steam header; HT, Low-pressure heater; HX, High-pressure turbine exhaust; IP, Intermediate-pressure turbine; LP, Low-pressure turbine; PP, Pipeline with a check valve; PT, Feedwater pump turbine; RE, Nuclear reactor; RH, Reheat steam generator; RT, Reheat turbine (1 intermediate and 2 low-pressure turbines); SG, Main steam generator; SX, Main steam generator discharge

Table 1 Comparison of steady-state model results with design data

Description	100% load		75% load		50% load	
	Model results	Heat balance data	Model results	Heat balance data	Model results	Heat balance data
Helium mass flowrate (lbm/sec)	5.174e+02	5.177e+02	4.108e+02	4.084e+02	2.920e+02	2.914e+02
Electrical generator output power (MW)	5.885e+02	5.800e+02	4.412e+02	4.350e+02	2.913e+02	2.900e+02
Normalized neutron flux (pu)	9.853e−01	9.800e−01	7.581e−01	7.607e−01	5.216e−01	5.200e−01
Feedwater mass flowrate (lbm/sec)	1.109e+03	1.116e+03	8.321e+02	8.368e+02	5.547e+02	5.564e+02
Feed pump pressure (psia)	3.195e+03	3.197e+03	2.854e+03	2.863e+03	2.608e+03	2.615e+03
Main steam pressure (psia)	2.415e+03	2.415e+03	2.415e+03	2.415e+03	2.415e+03	2.415e+03
Main steam temperature (F)	9.500e+02	9.500e+02	9.500e+02	9.500e+02	9.500e+02	9.500e+02
HP turbine impulse stage pressure (psia)	1.748e+03	1.750e+03	1.285e+03	1.290e+03	8.322e+02	8.400e+02
Mass flowrate through circulator turbine (lbm/sec)	3.559e+02	3.527e+02	2.208e+02	2.234e+02	1.336e+02	1.307e+02
Mass flowrate through turbine bypass valve (lbm/sec)	1.263e+01	1.590e+01	5.562e+01	5.264e+01	5.063e+01	5.269e+01
Hot reheat steam pressure (psia)	5.500e+02	5.500e+02	4.128e+02	4.140e+02	2.753e+02	2.760e+02
Hot reheat steam temperature (F)	1.000e+03	1.000e+03	1.000e+03	1.000e+03	1.000e+03	1.000e+03
Mass flowrate through IP turbine (lbm/sec)	1.106e+03	1.089e+03	8.292e+02	8.170e+02	5.528e+02	5.544e+02
LP turbine exhaust enthalpy (BTU/lbm)	1.032e+03	1.035e+03	1.050e+03	1.047e+03	1.076e+03	1.073e+03
Condenser pressure (psia)	1.125e+00	1.125e+00	1.125e+00	1.125e+00	1.125e+00	1.125e+00
Steam flowrate to lumped heater (lbm/sec)	1.839e+02	1.845e+02	1.246e+02	1.260e+02	7.127e+01	7.123e+01
Feed pump turbine steam mass flowrate (lbm/sec)	4.484e+01	4.500e+01	3.291e+01	3.280e+01	2.416e+01	2.400e+01
Feed pump turbine exhaust enthalpy (BTU/lbm)	1.079e+03	1.076e+03	1.103e+03	1.100e+03	1.131e+03	1.130e+03

controllability and observability, and to evaluate transfer function matrices. The details of these results are given in Ray[4]; only a part of the steady-state and transient performance is discussed here.

Steady-state solutions at different load levels in the range of 100–50% are given in *Table 1*; the results agree closely with the plant design data obtained from the manufacturers' specifications of individual components. This agreement partially established the validity of the model in the 50–100% load range. Complete model validation can only be obtained by comparison with field data which are not available. Generally, as base load units, nuclear power

plants are not expected to operate below 50% load; thus, the model is capable of simulating the real plant under normal operating conditions.

Dynamic response of a nonlinear system can be evaluated as long as it is stable in the test range. Transient responses of the (open loop, i.e. without controllers) nonlinear HTGR plant model were obtained for independent step disturbances in several input (control) variables from the equilibrium condition at 100% load; for illustrative purpose, some of them are presented in *Figures 2*, *3* and *4*. Each figure shows the responses of a particular system variable to a 5% step decrease in governor valve area, and to a 5% step increase in reactor control rod insertion (equivalent to an instantaneous reactivity change of −0.0012 unit). The step disturbances were applied at time t = 40 sec to display the steady-state condition before initiating disturbances. Dynamic responses were observed for an 800 sec period at 20 sec intervals.

Figure 2 shows the neutron flux transients with respect to the rated reactor capacity. For normal operation of the reactor, thermal fission power is directly proportional to neutron flux. A decrease in governor valve area increases flow resistance resulting in lower water/steam flow. However, governor valve area reduction has no significant effect on neutron flux. A slight decrease does result from a higher reactor core temperature due to negative feedback of temperature-induced reactivity associated with the fuel. Higher core, helium and steam temperatures follow the reduction in steam flow. Reactor rod insertion, on the other hand, abruptly reduces neutron flux due to the rod-induced prompt neutron reactivity reduction. Subsequently, as core temperature decreases, the neutron flux partially recovers due to negative temperature coefficient of reactivity. This effect overwhelms that of delayed neutron concentrations.

Main steam temperature transients are shown in *Figure 3*. Following a governor valve area reduction, feedwater flow decreases whereas reactor power remains

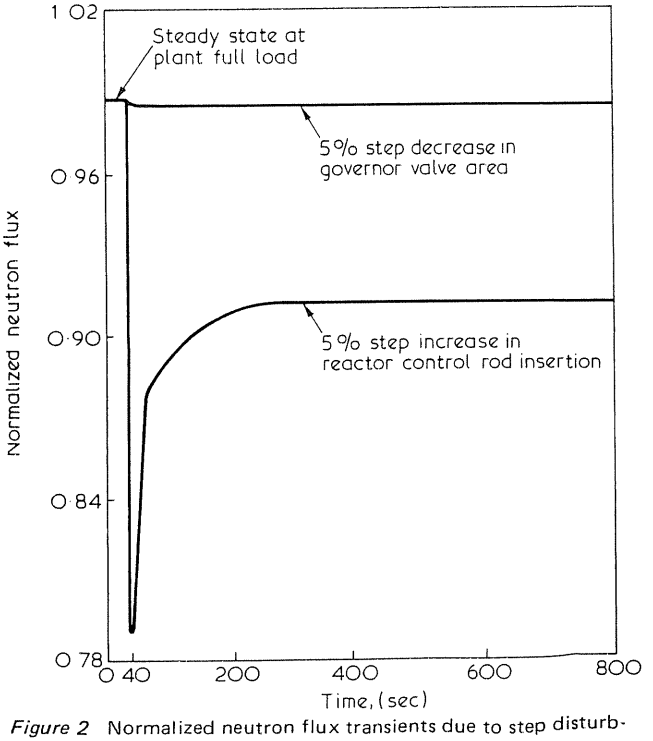

Figure 2 Normalized neutron flux transients due to step disturbances from full load

substantially constant (*Figure 2*). Main steam temperature increases because of a larger residence time of superheated steam in the main steam generator (due to longer superheater). In contrast, reactor rod insertion causing lower thermal fission power reduces main steam temperature.

Electrical power transients are shown in *Figure 4*. A decrease in governor valve area initially reduces electrical power due to a drop in high pressure turbine power. Within several minutes, the electrical power exceeds its original value due to improved thermal efficiency resulting from increased steam temperatures. A decrease in steam flow is overcompensated by increments in enthalpy differentials across the main steam turbines. On the other hand, with reactor rod insertion, electrical power decreases due to reduced thermal fission power and lower thermal efficiency resulting from lower steam temperatures.

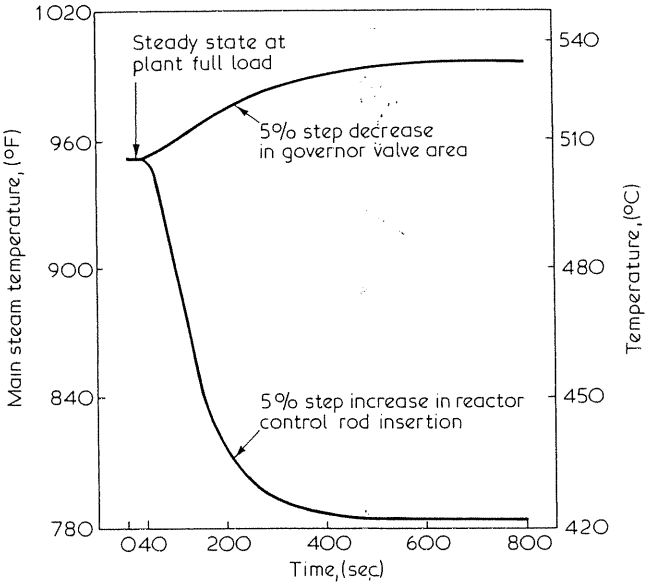

Figure 3 Main steam temperature transients due to step disturbance from full load

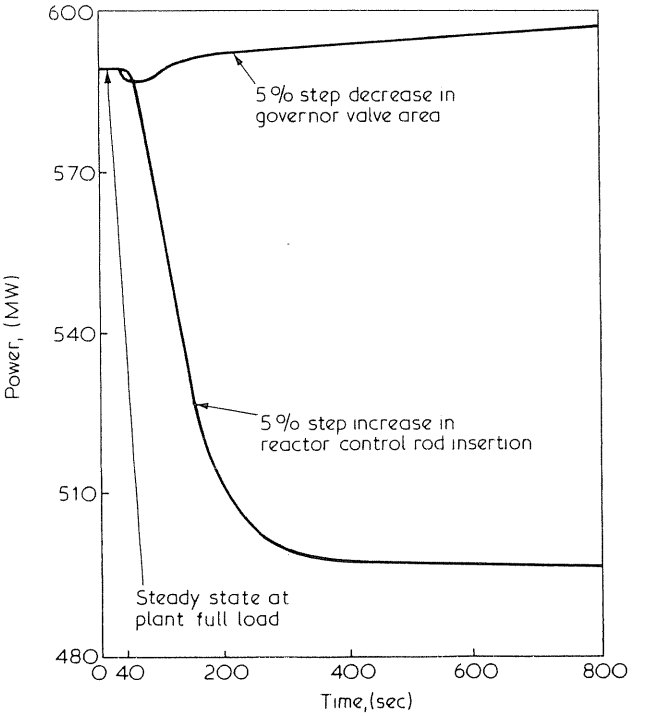

Figure 4 Electrical power transients due to step disturbances from full load

Conclusions

Modelling techniques and typical simulation results for a commercial scale HTGR steam power plant has been presented. The model results are useful for understanding complex and interactive process dynamics and also as a predictor of potential control and operational problems. In addition to controller design, the basic model structure can be extended to investigate the following: plant start-up and shutdown (normal and emergency), plant and operational safety procedures, and plant parameter sensitivity analyses, i.e. influence of heat transfer, fluid mechanic, and thermodynamic relationships on system performance.

References

1 *Nucl. News*, 1975, **18** (13), 21
2 Berkowitz, D. A. (Ed.). *Proc. Semin. Boiler Modeling*, The Mitre Corporation, Bedford, Massachusetts, October 1975
3 Broer, W. T. F. *et al.* Paper presented at *Joint IEEE/ASME Power Generation Tech. Conf.*, Miami Beach, Florida, 15–19 September 1974
4 Ray, A. *PhD Thesis*, Department of Mechanical Engineering, Northeastern University, Boston, Massachusetts (1976)
5 Adams, J. *et al. IEEE Trans. PAS*, 1965, PAS-84 (2), 146
6 Kwatny, H. G. *et al.* In *Prepr. Jt Autom. Control Conf.* 1971, pp. 227–236
7 McNamara, R. W. *et al.* In *Prepr. Jt Autom. Control Conf.* 1977, pp. 345–350

Appendix

List of state, output and input (control) variables

This state-space model has 40 state variables x, 11 output variables y, and five input variables u:

State variables x

Concentration of 1st lumped delayed neutron group
Concentration of 2nd lumped delayed neutron group
Average fuel temperature in upper half of reactor core
Average fuel temperature in lower half of reactor core
Average moderator temperature in upper half of reactor core
Average moderator temperature in lower half of reactor core
Steam pressure, upstream of circulator turbine bypass valve
Steam pressure at circulator turbine inlet
Steam density at circulator turbine exhaust
Specific steam enthalpy at circulator turbine exhaust
Circulator turbine-compressor shaft speed
Helium temperature at compressor inlet
Helium temperature at reactor lower plenum
Economizer length in main steam generator
Average specific internal energy of compressed water in economizer
Average tube wall temperature in economizer at mean radius
Economizer-evaporator length
Average tube wall temperature in evaporator at mean radius
Density of saturated steam at evaporator-superheater boundary
Average specific internal energy of steam in superheater
Average tube wall temperature in superheater at mean radius
Average specific enthalpy of steam in reheat steam generator
Average tube wall temperature in reheat steam generator at mean radius
Steam density at main steam generator discharge
Specific steam enthalpy at main steam generator discharge
Main (throttle) steam pressure
Steam pressure downstream of wide open governor valves
Steam pressure downstream of partially open governor valves
Steam pressure at high-pressure turbine impulse stage
Steam density at high-pressure turbine exhaust
Specific steam enthalpy at high-pressure turbine exhaust
Steam density at hot reheat header
Specific steam enthalpy at hot reheat header
Steam pressure at intermediate pressure turbine extraction
Steam pressure at low-pressure turbine lumped extraction
Saturated water temperature in the lumped heater shell
Feedwater pump-turbine shaft speed
Specific enthalpy of saturated water in deaerator storage tank
Feedwater flow
Specific enthalpy of feedwater at main steam generator inlet

Output variables y

Feedwater flow
Feedwater pump-turbine shaft speed
Main (throttle) steam pressure
Main (throttle) steam temperature
Steam pressure at high-pressure turbine impulse stage
Steam pressure upstream of circulator turbine bypass valve
Steam pressure at helium circulator turbine exhaust
Circulator turbine-compressor shaft speed
Hot reheat steam temperature
Normalized neutron flux
Electrical power

Input variables u

Governor valve area
Reactor control rod insertion
Circulator turbine control valve area
Circulator turbine bypass valve area
Feed pump turbine control valve area